Российская Академия Наук

РОССИЙСКАЯ АКАДЕМИЯ НАУК

ИНСТИТУТ ПРОБЛЕМ БЕЗОПАСНОГО РАЗВИТИЯ АТОМНОЙ ЭНЕРГЕТИКИ

RUSSIAN ACADEMY OF SCIENCES

NUCLEAR SAFETY INSTITUTE

Препринт ИБРАЭ № IBRAE-1998-11

Preprint IBRAE-1998-11

M.S. Veshchunov

DEVELOPMENT OF THE THEORY OF FISSION GAS BUBBLE EVOLUTION IN IRRADIATED UO_2 FUEL

Москва 1998

Moscow 1998

УДК

Вещунов М.С. РАЗВИТИЕ ТЕОРИИ ЭВОЛЮЦИИ ГАЗОВОЙ ПОРИСТОСТИ В ОБЛУЧЕННОМ UO_2 ТОПЛИВЕ. Препринт № IBRAE-98-11. Москва. Институт проблем безопасного развития атомной энергетики РАН. Июль 1998. 15 с. — Библиогр.: 33 назв.

Аннотация

В настоящей работе на базе имеющихся экспериментальных данных представлен критический анализ стандартных подходов при моделировании развития внутри зеренной и межзеренной пористости в UO_2 топливе. Показано, что главным источником ошибок стандартных моделей являются недооценка радиационных эффектов при низких температурах (ниже 1500°C) и тепловых эффектов при высоких температурах (выше 1500°C). Представленный анализ позволяет количественно описать процессы нуклеации пузырей, их диффузионного роста, а также вычислить размер и концентрацию внутризеренных пузырей, установившиеся в условиях стационарного облучения.

Veshchunov M.S. DEVELOPMENT OF THE THEORY OF FISSION GAS BUBBLE EVOLUTION IN IRRADIATED UO_2 FUEL. Preprint IBRAE-98-11. Moscow. Nuclear Safety Institute. Jule 1998. 15 p. — Refs.: 33 items.

Abstract

In the present paper the standard approaches for modelling of the inter- and intragranular bubbles evolution in the UO_2 fuel are critically analyzed on the basis of available experimental data. It is demonstrated that the main source of errors in the simplified treatment of the problem by the standard models can be associated with underestimation of the radiation effects at low temperatures (below 1500°C) and thermal effects at high temperatures (above 1500°C). The presented analysis allows quantitative description of the bubble nucleation mechanism, adequate modelling of the bubble diffusional growth, and evaluation of the intragranular bubble number density and stable size attained under steady irradiation conditions.

Development of the Theory of Fission Gas Bubble Evolution in Irradiated UO_2 Fuel

M.S. Veshchunov

Nuclear Safety Institute (IBRAE), Russian Academy of Sciences

B.Tul'skaya, 52, Moscow, 113191

phone: (095) 955 2618, fax: (095) 958 0040, e-mail: vms@ibrae.ac.ru

I. Introduction

The influence of fission gases generated in oxide fuels during irradiation on fuel performance has been the subject of many investigations over the past 40 years. The fission inert gases are known to precipitate into bubbles. The growing bubbles cause the fuel to swell. In addition, fission gas bubbles retained in the fuel on grain surfaces and edges can cause radical changes in the fuel microstructure. These changes in the fuel microstructure can then result in an enhanced gas release and fuel swelling.

Any model that attempts a realistic description of fission gas release and swelling as a function of fuel-fabrication variables and a wide range of reactor operating conditions must treat fission gas release and fuel swelling as coupled phenomena and must include many mechanisms influencing fission gas behaviour. Currently, the most advanced models which include mechanistic description of these phenomena are the numerical codes GRASS-SST [1], FASTGRASS [2], VICTORIA [3]. These codes consider the effects of production of gas from fissioning uranium, bubble nucleation, a realistic equation of state for xenon, lattice gas diffusivities based on experimental observations, bubble growth, migration and coalescence, re-solution, temperature and temperature gradients, interlinked porosity, etc.

However, some of the basic models of the codes seem to be oversimplified and do not allow realistic description of many observed phenomena. The basic assumption of these models is connected with the bubble state description by the so called «capillarity» relation and the quasi-stationary approximation for the bubble growth based on this relation. Such an approach radically simplifies the theory, since in this case the defect structure of the crystal (including point defects, such as vacancies and interstitials, and extended defects, such as dislocations) is practically excluded from consideration (with the exception of some simple effects such as athermal behaviour of the gas and uranium atom diffusivities in the irradiated crystal). However, this consideration is well grounded only for the description of equilibrium crystals and generally fails under irradiation conditions when the fuel matrix is oversaturated with the point defects (vacancies and interstitials).

In parallel to the fuel behaviour investigations, extensive experimental and theoretical studies of metal crystal behaviour under irradiation conditions were carried out (e.g. [4-6]). Results of these investigations unambiguously demonstrated a great influence of point defects generated under similar (to the fuel) irradiation conditions on the bubble nucleation and growth in metals. However, these results were mainly unaccounted in the models dealing with the bubble porosity evolution in the oxide fuel, despite the general character of many theoretical conclusions.

In the present paper an attempt is made to extend the general approach of the irradiated metal description to the modelling of the bubble behaviour in the UO_2 fuel. It is demonstrated that in some cases the standard approach for the bubble behaviour in the fuel (based on the capillarity relation) can be really used (for example, at high temperatures above 1500°C), however, in other cases a more realistic description of bubble interactions with non-equilibrium point defects must be applied. Hence, the radiation effects unaccounted in the models [1-3] become especially important in the case of the large bubbles evolution (observed on the grain faces and, after temperature transients, in the bulk of the grains), since in these cases the mechanism and rate of the fuel swelling and gas release through the open porosity may be strongly underestimated by the standard approach (see sections II and V).

Naturally, a similar to the metal description approach leads sometimes to quite different results for the fuel, since many parameters of the two systems differ significantly. For example, the mechanism of small bubble

interactions with fission fragments in the fuel, associated with the bubble relaxation in the short living (~ 10^{-11} s) molten zone of fission tracks (considered in section II), can strongly change the intragranular porosity evolution. Or, a relatively small value of the self-diffusion coefficient in the fuel (in comparison with that in metals) leads to a significant extension of the initial, so called «recombination» stage of irradiation when the main sink of point defects is their mutual recombination. As a result, this allows the direct calculation of the bubble nucleation factor (determined in the codes [1-3] as a default value varying in a wide range), or a natural explanation of the stabilisation of the bubble number density observed under steady irradiation conditions at $T \leq 1500$°C and its self-consistent calculation (section III).

On the other hand, in the case of high temperatures (≥ 1500°C) when radiation effects in the fuel can be mainly neglected, the codes [1-3] generally underestimate thermal effects in the fuel, namely, do not consider the thermal resolution of gas atoms from bubbles. These effects strongly influence the bubble nucleation mechanism which at these temperatures becomes associated with the fluctuation formation of a finite size critical nucleus, as well as the bubble evolution in a late stage of irradiation when the thermal resolution apparently determines the observed stabilisation of the bubble number density (section IV).

II. Intragranular porosity: general consideration

II.1. Standard approach

In the majority of the currently existing models for the fission gas behaviour in the UO_2 fuel, mechanical equilibrium state with respect to surface capillary forces of bubbles expressed by the capillarity relation:

$$P - P_h = 2\gamma/R, \tag{1}$$

where P is the internal gas pressure, P_h is the external hydrostatic pressure, R is the radius of the bubble, γ is the surface energy, is the usual approximation for the description of the growing intragranular bubbles (e.g. see [1-3, 7-9]). In the case of the deviation from this state, for example, due to coalescence of two bubbles, it is proposed that the newly formed bubble quickly attains the equilibrium state after some characteristic relaxation time by the vacancy diffusion mechanism. This approach is usually based on the kinetic equation for the diffusional growth of bubbles [10]:

$$dR/dt = (D_u/R)\{1 - \exp[(P - P_h - 2\gamma/R)\Omega/kT]\}, \tag{2}$$

where $D_u \approx D_v c_v$ is the U atom self-diffusion coefficient, D_v and c_v are the vacancy diffusion coefficient and bulk concentration, respectively; Ω is the atomic volume in the UO_2 matrix ($\Omega \approx 4.1\times10^{-23}$ cm^3). In accordance with Eq. (2) the quasi-stationary state of a bubble ($dR/dt = 0$) is characterised by the capillarity relation, Eq. (1).

II.2. Correct description

However, such an approach becomes incorrect in many cases since Eq. (2) is valid only for the equilibrium crystals, i.e. when the concentration c_v of vacancies does not exceed the thermal equilibrium value c_v^{eq}. Otherwise, for crystals oversaturated with the non-equilibrium vacancies more adequate expression has the form [11]:

$$dR/dt = (D_u/R)\{1 - (c_v^{eq}/c_v)\exp[(P - P_h - 2\gamma/R)\Omega/kT]\}, \tag{3}$$

thus, the capillarity relation, Eq. (1) does not anymore correspond to the quasi-stationary state ($dR/dt = 0$) if (c_v^{eq}/c_v) << 1. Moreover, under irradiation conditions the bubble growth is determined also by the diffusion of the non-equilibrium interstitials and the correct expression takes the form [4,5]:

$$dR/dt = (D_u/R)\{1 - (\beta_i/\beta_v) - (c_v^{eq}/c_v)\exp[(P - P_h - 2\gamma/R)\Omega/kT]\}, \tag{4}$$

where $\beta_i = D_i/c_i$, $\beta_v = D_v/c_v$; D_i and c_i are the interstitial diffusion coefficient and bulk concentration, respectively.

This equation can be also rewritten in the form:

$$dx/dt = D_u x^{1/3} (3\Omega/4\pi)^{-2/3}(1 - \beta_i/\beta_v)\{1 - (c_v^{eq}/c_v)(1 - \beta_i/\beta_v)^{-1}\exp[(P - P_h - 2\gamma/R)\Omega/kT]\}, \quad (5)$$

where x is the amount of vacancies comprising the void, i.e. $x = (4/3)\pi R^3/\Omega$.

As it will be shown below, at T < 1500°C the value of (c_v/c_v^{eq}) attains several orders of magnitude (e.g. $(c_v^{eq}/c_v) \approx 10^{-4}$ at T = 1000°C), whereas $(1 - \beta_i/\beta_v) \approx 10^{-2}$. Therefore, application of the capillarity relation, Eq. (1) becomes invalid under these conditions, since the quasi-stationary state of a bubble ($dR/dt = 0$) derived from Eq. (5) corresponds to a new relation:

$$(P - P_h - 2\gamma/R)\Omega = - kT \ln[(c_v/c_v^{eq})(1 - \beta_i/\beta_v)], \quad (6)$$

At 1000°C the difference between $\Delta P = P - P_h$ and the capillary pressure $2\gamma/R$ attains $\approx 10kT/\Omega \approx 10$ GPa (!), and continues to increase with the temperature decrease (along with the increase of (c_v/c_v^{eq})).

At T ≥ 1500°C , as shown below, the radiation induced concentration c_v really does not exceed the thermal equilibrium value c_v^{eq}, thus, Eq. (2) becomes valid at high temperatures. However, at T ≤ 1500°C application of Eq. (4) instead of Eq. (2) for the bubble growth can strongly change the kinetics of the intragranular porosity evolution.

In order to demonstrate this statement, it is sufficient to consider the behaviour of a solely growing bubble during a time interval between two subsequent collisions with other bubbles. It should be noted that the Brownian mobility of bubbles is considered in many theoretical papers to be significant (mainly on the basis of observations [12]), leading to relatively high frequency of mutual collisions. However, in the subsequent tests [13] it was clearly demonstrated, that at T ≤ 1800°C the Brownian motion of bubbles is negligibly slow, therefore, the time between two subsequent collisions of a bubble (in the absence of temperature gradients in the grain) is really very large. In this case the analysis of the behaviour of growing bubbles can be performed on the basis of Eqs. (2) or (5) along with a corresponding kinetic equation for the number of gas atoms N in a bubble:

$$dN/dt = D_g c_g (3\Omega/4\pi)^{-2/3} x^{1/3} [1 - NK_g/(D_g c_g x^{1/3})], \quad (7)$$

where D_g and c_g are the gas atom diffusion coefficient and bulk concentration, respectively; K_g is the rate of the radiation induced resolution of gas atoms from a bubble; and with the Van-der-Waals equation of state:

$$P(x\Omega - bN) = NkT, \quad (8)$$

where $b \approx 8.5\times10^{-23}$ cm^3/atom is the Van-der-Waals constant.

It should be noticed, however, that Eq. (7) based on the usual consideration of the gas subsystem in the models [1-3], lacks a term corresponding to the thermal resolution of gas atoms from bubbles. Neglecting of such a term is often grounded, however, in many important cases does not allow correct description of the system behaviour (in particular, at T > 1500°C, as shown below in section IV).

II.3. Qualitative analysis of bubble evolution

It is rather illuminating to perform analysis of the two differential equations (in the simplest case, Eqs. (2) and (7)) in terms of the phase portrait of the system, Fig.1 (compare with [14]). Intersection of two nodal lines $dx/dt = 0$ and $dN/dt = 0$ determines a critical point I of the stable node type, i.e. particles (gas atoms (N) and vacancies (x)) move toward the node from all quadrants in the neighbourhood. In the case of applicability of the ideal gas law (instead of more realistic Eq. (8)) the nodal lines are described by relationships $N \propto x^{2/3}$ and $N \propto x^{1/3}$, respectively. The critical point apparently determines parameters of stable bubbles and explains the validity of the «bimodal» bubble size distribution, observed in the steady state tests and usually represented by the models based on Eqs. (2) and (7). When a bubble deviates from this stable state, diffusion fluxes of the gas atoms and point defects arise which return the bubble back to the initial state.

In the case when Eq. (2) is substituted by Eq. (5) the nodal line $dx/dt = 0$ is described by the equation:

$$N = (4\pi/3)^{1/3}(2\gamma/kT)(x\Omega)^{2/3} - kT \ln[(c_v/c_v^{eq})(1 - \beta_i/\beta_v)],$$

and changes its form with temperature decrease, Fig.2 (for the sake of simplicity the ideal gas law is used here instead of Eq. (8)). At some temperature below 1500°C the second critical point II (of the saddle type) appears which can be reached from the first critical point only due to thermal fluctuations and/or collisions of bubbles. Along with the further temperature decrease the two points approach to each other and finally disappear. For the above presented values of the parameters $(c_v^{eq}/c_v) \approx 10^{-4}$ and $[1 - (\beta_i/\beta_v)] \approx 10^{-2}$ attained at T=1000°C, the critical points are knowingly absent, Fig.3. In this situation bubbles grow unrestrictedly (along the dashed line in Fig.3), this is generally in contradiction with observations [15-18], which evidence that in the reactor steady operation regimes in a wide temperature interval (from 600 to 1800°C) the size of the bubbles stabilise ($R \approx$ 5-10 Å) in some period of time.

II.3.a. Small bubble relaxation mechanism

The main reason for this discrepancy of the theory with observations is connected with an unaccounted additional physical mechanism of bubble interactions with fission fragments. Up-to-now such interactions were considered only in the equation for the gas subsystem (i.e. Eq. (7)) in the form of the radiation induced resolution of gas atoms from bubbles. However, one should also take into consideration interactions of fission fragments with vacancy subsystem which becomes especially important for small bubbles ($R \approx 10$ Å). Indeed, in accordance with the contemporary microscopic theory of the material interactions with high energy fission particles (see, for example, [19]), molten zones appear in the fission fragment tracks during some short time interval $\tau^* \sim 10^{-11}$ s. Despite an apparent smallness of this time interval, it appears to be large enough for high temperature annealing of a small bubble with $R \approx 10$ Å and its (partial) relaxation to the equilibrium state in the molten zone of the track with diameter ≈ 70-100 Å. Such a state in the liquid phase is a mechanically equilibrium bubble described by the capillarity relation, Eq. (1), and the relaxation time to this state can be estimated as $\tau_r \sim R/v_s$, where v_s is the sound velocity in the melt. [This estimation can be deduced in a similar way to the solution of the problem of an empty void shrinkage in the incompressible liquid [20] by generalisation to the case of a gas filled void]. Assuming $v_s \sim 10^3$ m/s, $R \approx 10$ Å, one gets $\tau_r \sim 10^{-12}$ s $\leq \tau^*$.

The simplest way to account for this mechanism is the introduction in Eq. (5) of an additional term, describing bubble relaxation as a result of its collisions with fission fragments. Under an assumption that the path volume V_{tr} is equal to $\pi r_{tr}^2 L$, where $r_{tr} \approx 50$ Å, $L \approx 6\times10^{-4}$ cm are the track radius and length, respectively, a mean time between collisions of a small bubble with particles is estimated as $\tau_0 \sim (V_{tr}F)^{-1} \sim 10^2$ s, where $F \approx 10^{13}$ s^{-1}cm^{-3} is the fission rate. Correspondingly, an additional term $K_v(x - x_L(N))$ is introduced in Eq. (5), where $K_v \propto \tau_0^{-1}$, and $x_L(N)$ corresponds to the capillarity relation expressed in terms of the values x and N. In the considered case of small overpressurised bubbles with $R \leq 10$ Å this relation is completely determined by the Van-der-Waals constant $b \approx 8.5\times10^{-23}$ cm^3 and can be reduced to the form $x_L(N) \approx (b/\Omega)N \approx 2N$. A proportionality factor in the relation $K_v \propto \tau_0^{-1}$ may significantly differ from 1 reflecting the probability of incomplete relaxation of a bubble during short-term ($\tau^* \sim 10^{-11}$ s) annealing in the molten zone of a track. Finally, one gets instead of Eq. (5):

$$dx/dt = D_u (3\Omega/4\pi)^{-2/3} x^{1/3}(1 - \beta_i/\beta_v)\{1 - (c_v^{eq}/c_v)(1 - \beta_i/\beta_v)^{-1}\exp[(P - P_h - 2\gamma/R)\Omega/kT]\} - K_v(x - x_L(N)). \quad (9)$$

Analysis of Eq. (9) shows that the additional term in the r.h.s. recreates the critical point at the intersection of the two nodal lines $dx/dt = 0$ and $dN/dt = 0$ and, thus, leads to the stabilisation of the bubble radius in the steady stage of irradiation also in the case of low temperatures (see Fig.4).

II.3.b. Large bubble evolution

It should be emphasised, however, that the above proposed mechanism of a small bubble annealing becomes invalid for bubbles with the diameter exceeding the width of the fission particle tracks (~100 Å). Under steady irradiation conditions this limitation is insignificant, since radii of the bubbles are stabilised and do not exceed ≈ 10 Å. Under transient conditions the situation can radically change. For example, it was observed in the tests [21] that during a power transient the fuel temperature rises rapidly, leading to the growth of large (10 to 500 nm diameter) fission gas bubbles. Such large bubbles cannot be annealed in the molten zone of tracks and probably

conserve their dimension x or reduce it but essentially less effectively (for example, by the vacancy radiation resolution mechanism similar to the above discussed gas atom resolution from bubbles). In this case the system behaviour is again described by the phase portrait similar to Fig.3, i.e. large bubbles (with $R >> 50$ Å) formed during the transient period grow up unrestrictedly.

Since in this case (in the absence of restrictions implied by the capillarity relation, Eq. (1)) the gas atom diffusion is not anymore the rate determining step of the bubble growth kinetics, on the one hand, and owing to a relatively small value of the gas atom flux to the growing bubble ($\propto D_g c_g$) in comparison with the effective flux of point defects ($\propto D_u (1 - \beta_i/\beta_v)$), on the other hand, bubbles become essentially depressurised and grow up very rapidly (along the dashed line in Fig.3) in comparison with the usually proposed evolution (along the nodal line $dx/dt = 0$). In particular, this may lead to the significantly larger and quicker swelling of the fuel than usually expected.

III. Irradiation effects

Essential factors determining the system behaviour and entering in Eq. (3) are the non-equilibrium point defect concentrations c_v (vacancies) and c_i (interstitials). For their calculation one can use the rate theory continuum model of Brailsford and Bullough [22]:

$$dc_v/dt = K + K_e - D_v c_v k_v^2 - \alpha D_i c_i c_v ,$$

$$dc_i/dt = K - D_i c_i k_i^2 - \alpha D_i c_i c_v , \qquad (10)$$

where K is the atomic displacement rate (usually proposed $\approx 10^{-5}$ s^{-1} for the PWR reactor normal operation conditions), K_e is the rate of thermal vacancy production, $k_{v(i)}^2$ is the sink strength for vacancies (interstitials), α is the recombination constant ($\approx 4\pi r_c/\Omega$, where $r_c \approx$ 1-5 Å).

If voids and dislocations are the only fixed sinks:

$$k_v^2 = 4\pi\rho_b R + Z_v\rho_d ,$$

$$k_i^2 = 4\pi\rho_b R + Z_i\rho_d , \qquad (10')$$

where ρ_b and ρ_d are the void number and dislocation density, respectively; the dislocation sink strength constants Z_v and Z_i for vacancies and interstitials are the order of unity, but Z_i is a few percent larger due to the greater elastic interaction between dislocations and interstitials, than with vacancies.

For calculation of the bulk concentrations c_v and c_i, the grain boundary sink strength $k_{g.b.}^2$ can be neglected in comparison with the bulk sinks $k_{v,i}^2$, since

$$k_{g.b.}^2 / k_{v,i}^2 \approx 3/(R_g k_{v,i}) << 1,$$

where R_g is the grain radius.

In the steady state ($dc_v/dt = dc_i/dt = 0$) the general solution of Eqs. (10) is:

$$c_i = (D_v k_v^2/2\alpha)[-(1 + \mu) + ((1 + \mu)^2 + \eta)^{1/2}],$$

$$c_v = (D_i k_i^2/2\alpha)[-(1 - \mu) + ((1 + \mu)^2 + \eta)^{1/2}], \qquad (11)$$

where $\eta = 4\alpha K/(D_v k_i^2 k_v^2)$, $\mu = K_e\eta/(4K)$.

III.1. Low temperatures, T ≤ 1500°C

As it will be demonstrated below, at T ≤ 1500°C $K_e << K$; on the other hand, η occurs to be rather large (>> 1) during a very long initial stage of the steady state period of irradiation. Indeed, at T ≈ 1000°C $D_v \approx 10^{-11}$ cm^2/s

(see below Eq. (14) and/or compare with data presented in [23]), and the relationship $\eta >> 1$ is valid until the parameters k_i^2, k_v^2 attain the value $\approx 10^{11}$ - 10^{12} cm^{-2}, i.e. practically up to the maximal observed number density of the bubbles (with $R \leq 10$ Å), $\rho_b \approx 10^{17}$ - 10^{18} cm^{-3}. At higher temperatures (up to 1500°C) this relationship is valid in a slightly reduced range of the parameters $k_{v,i}^2$ variation (up to $\approx 10^{10}$ - 10^{11} cm^{-2}) owing to some increase of D_v. At lower temperatures (below 1000°C) the uranium self-diffusion coefficient D_u becomes completely athermal and independent on temperature, $D_u \approx 10^{-16}$ cm^2/s (at the fission rate $F \approx 10^{13}$ cm^{-3}s^{-1} [23, 24]). As shown below (Eq. (14)), D_v becomes also temperature independent and, thus, the applicability range of the relationship $\eta >> 1$ does not reduce. This is a rather important conclusion, since in this case the general solution, Eq. (11) can be radically simplified:

$$c_v \approx (K\Omega k_i^4/4\pi r_c\, k_v^2 k_i^2 D_v)^{1/2} \approx (K\Omega/4\pi r_c D_v)^{1/2},$$

$$D_i c_i \approx D_v c_v (k_v^2/k_i^2), \qquad (12)$$

i.e. c_v, c_i become practically independent on the amount of voids and dislocations in the crystal, since the mutual recombination of the point defects dominates in this stage. Owing to $D_u \approx D_v c_v \approx D_i c_i$, finally one gets:

$$c_v \approx K\Omega/4\pi r_c D_u, \qquad (13)$$

$$D_v \approx 4\pi r_c D_u^2/K\Omega. \qquad (14)$$

Correspondingly, at T ≤ 1000°C ($D_u \approx 10^{-16}$ cm^2/s) one gets $c_v \approx 10^{-5}$, $D_v \approx 10^{-11}$ cm^2/s. At higher temperatures (up to 1500°C) D_u slowly increases up to its thermal value at 1500°C, $D_u \approx 10^{-15}$ cm^2/s. Therefore, the calculated value of c_v reduces to $\approx 10^{-6}$, i.e. c_v attains its equilibrium value at 1500°C, $c_v^{eq} \approx \exp(-2.2\ \text{eV}/kT) \approx 6\times10^{-7}$ [23].

III.1.a. Nucleation factor

It is important to notice that Eq. (13) allows the calculation of the so called nucleation factor F_N, introduced in many models as a default value (usually varying in a wide range 10^{-4} - 10^{-7}) to determine the probability that two gas atoms that have come together actually stick and form a bubble [1-3]. Indeed, it is easy to understand that for the stability of such a bubble at least one vacancy must be located in the position of the two atoms collision; otherwise, the formed bubble will immediately disintegrate. [Formally in terms of Eq. (8) it is directly seen that the bubble with $x = 0$ (no vacancies) and $N = 2$ corresponds to the non-physical state with the negative pressure P]. On the other hand, the probability that a vacancy is located in a certain position is exactly equal to the vacancy bulk concentration c_v, which can be deduced from Eq. (13):

$$F_N = c_v \approx K\Omega/4\pi r_c D_u. \qquad (13')$$

Therefore, at T ≤ 1000°C

$$F_N \approx 10^{-5} \times (F/F_0), \qquad (15)$$

where F is the fission rate, $F_0 = 10^{13}$ cm^{-3}s^{-1}, and at higher temperatures (up to 1500°C) F_N smoothly reduces by one order of magnitude:

$$F_N \approx 10^{-6} \times (F/F_0). \qquad (15')$$

III.1.b. Sink strengths

In order to calculate the parameter $(1 - \beta_i/\beta_v)$ at T < 1500°C which at these temperatures is equal to $1 - (k_v^2/k_i^2)$ (see Eq. (12)) and, thus, becomes a small value (<< 1), one should take into account that in this case an additional problem of calculation of the dislocation density ρ_d (determining the dislocation sink strength $Z_{i,v}\rho_d$) arises. In the initial stage of irradiation, when the bubble number density ρ_b is low whilst the dislocation density is finite and determined by the original state of the crystal (usually estimated as $\rho_d \approx 10^8$ cm^{-2}), $4\pi\rho_b R << Z_{i,v}\rho_d$, therefore, one gets from Eq. (10') $k_i^2 \approx Z_i\rho_d$, $k_v^2 \approx Z_v\rho_d$, and $1 - \beta_i/\beta_v \approx 1 - Z_v/Z_i \approx 10^{-2}$.

Along with the irradiation dose increase, the bubble number density ρ_b and dislocation density ρ_d simultaneously increase. While the bubble sink strength $4\pi\rho_b R$ does not exceed the dislocation sink strength $Z_{i,v}\rho_d$, the value $1 - \beta_i/\beta_v$ remains the same. From the analysis of the equation for the radius R_L of the growing interstitial dislocation loops (with the Burgers vector b) [25]:

$$dR_I/dt \approx b^{-1}(Z_i D_i c_i - Z_v D_v c_v) \approx b^{-1} Z_v D_v c_v [(Z_i/Z_v)(k_v^2/k_i^2) - 1],$$

it is straightforward to see that until $4\pi\rho_b R << Z_{i,v}\rho_d$ is valid (i.e. $k_i^2 \approx Z_i\rho_d$, $k_v^2 \approx Z_v\rho_d$), the dislocation loop growth is strongly suppressed (with respect to the bubble growth):

$$dR_I/dt \propto [(Z_i/Z_v)(Z_v/Z_i) - 1] \to 0.$$

In the opposite case of a large number density of bubbles, $4\pi\rho_b R >> Z_{i,v}\rho_d$, and $k_i^2 \approx k_v^2 \approx 4\pi\rho_b R$, the bubble growth turns to be suppressed (with respect to the loop growth), since from the equation for the growing bubble radius:

$$dR/dt \approx R^{-1}(D_v c_v - D_i c_i),$$

in this case one can deduce:

$$dR/dt \approx R^{-1} D_v c_v (1 - k_v^2/k_i^2) \to 0.$$

Therefore, it is logically to assume that after some time the relationship $4\pi\rho_b R \approx Z_{i,v}\rho_d$ becomes valid, and the further growth of the bubbles and dislocation loops occurs self-consistently, in accordance with this relationship. In this case $1 - \beta_i/\beta_v$ remains $\approx 10^{-2}$. Indeed, this conclusion can be selectively confirmed by some data found in the literature. For instance, in the test [21] both densities ρ_b and ρ_d were measured after some period of the steady irradiation: $\rho_b \approx 10^{16}$ cm^{-3}, $\rho_d \approx 10^{10}$ cm^{-2}, and the mean bubble radius $R \approx 4$ nm, thus, the approximate equation $4\pi\rho_b R \approx Z_{i,v}\rho_d$ was really valid.

After completion of the «recombination stage», $\eta \geq 1$ and dislocations and bubbles become the main sinks determining the steady state concentration of the point defects, i.e. Eq. (12) becomes invalid. As already mentioned, the transition to the new regime at T ≤ 1500°C occurs at a late stage of the steady irradiation, when the bubble number density attains $\rho_b \approx 10^{17} - 10^{18}$ cm^{-3}. In the new regime $\eta >> 1$ and the general solution Eq. (11) can be reduced to the form:

$$c_v \approx K/k_v^2 D_v, \qquad \text{or} \qquad K \approx k_v^2 D_v c_v \approx k_v^2 D_u. \tag{16}$$

As already mentioned, at T≤ 1000°C D_u depends only on the fission rate F and does not depend on temperature: $D_u \approx 10^{-16} - 10^{-17}$ cm^2/s. At higher temperatures (up to 1500°C) D_u smoothly increases up to 10^{-15} cm^2/s. Therefore, k_v^2 attains the steady value also in the new regime. This value determined by Eq. (16) weakly depends on temperature, being $k_v^2 \approx 10^{11} - 10^{12}$ cm^{-2} at T ≤ 1000°C and smoothly reducing to $k_v^2 \approx 10^{10} - 10^{11}$ cm^{-2} at T ≤ 1500°C. Moreover, in all these cases k_v^2 does not exceed the value attained in the recombination stage.

This means that the value of k_v^2 attained at T ≤ 1500°C in the recombination stage is practically final and does not increase anymore during the subsequent stage. Since $k_{v,i}^2 = 4\pi\rho_b R + Z_{v,i}\rho_d$, and, as shown above, $4\pi\rho_b R \approx Z_{i,v}\rho_d$, then the attained stabilised value of the bubble number density is $\rho_b \approx 10^{17} - 10^{18}$ cm^{-3}, in a fair agreement with experimental data for the bubble number density observed in the steady stage of irradiation [15-18].

III.2. High temperatures, T ≥ 1500°C

At T ≥ 1500°C the thermal effects dominate over radiation ones, $K_e \geq K$, and the general solution, Eq. (11), self-consistently transforms into

$$c_v \approx c_v^{eq} \approx K_e/k_v^2 D_v, \qquad D_i c_i \approx D_v c_v (k_v^2/k_i^2)(K/K_e) << D_v c_v, \tag{17}$$

therefore, $1 - \beta_i/\beta_v = 1 - (D_i c_i/D_v c_v) \approx 1$.

In contrast with the low temperature case, Eq. (17) does not imply any limitations to the value of k_v^2. Therefore, additional (thermal) mechanisms should be considered in order to explain the observed stabilisation of this parameter at high temperatures.

IV. Thermal resolution of gas atoms

As already mentioned, an additional term representing the thermal resolution of gas atoms from bubbles is usually not considered in the equation describing the behaviour of the gas subsystem (i.e. Eq. (7)). It will be demonstrated here that namely such a process determines the mechanism of the bubble nucleation and becomes responsible for the observed stabilisation of the bubble number density at T ≥ 1500°C.

A comprehensive analysis of this process should be carried out with the account of the non-ideal state of the overpressurised gas in small bubbles ($R \approx 10$ Å), since Van-der-Waals corrections are especially influential in terms of this thermal process. However, for a qualitative analysis of the system behaviour, the problem may be simplified in the ideal gas approximation. Numerical calculations for the non-ideal gas (which will be published elsewhere) generally confirm the main qualitative conclusions derived from the analysis of the simplified problem.

In the ideal gas approximation the account of the thermal resolution of gas atoms from a bubble transforms Eq. (7) into the following one:

$$dN/dt = D_g c_g (3\Omega/4\pi)^{-2/3} x^{1/3}[1 - NK_g/(D_g c_g x^{1/3}) - NkT/x\Omega P_e], \quad (18)$$

where P_e is the gas pressure in the bubble in equilibrium with the solid solution of the gas atoms in the fuel matrix. Assuming Henry's law behaviour up to the terminal solubility c_s, one gets $P_e = (P_s/c_s)c_g$. However, the ratio (P_s/c_s) is unknown, thus, it can be only roughly evaluated from the available indirect data. Hence, it is known from the literature [26] that the solubility of He in UO_2 measured in the pressure range 5-10 MPa at 1200°C, yields $(P_s/c_s) \approx 1.5\times10^{12}$ Pa. This value will be used hereafter for quantitative estimations, bearing in mind that for Xe and Kr it can be somewhat different and also temperature dependent (Arrhenius law).

IV.1. Qualitative analysis of the system behaviour

The first conclusion which can be drawn from the analysis of Eq. (18) is that at high temperatures (T ≥ 1500°C) the thermal resolution term (the third one in the r.h.s.) dominates over the radiation induced resolution term (the second one in the r.h.s.). Indeed, the ratio q of these terms is equal to $D_g kT/[K_g\Omega^{5/3}(P_s/c_s)x^{2/3}]$ and increases with the increase of the gas atoms diffusion coefficient D_g. At T ≈ 1500°C, $D_g \approx 10^{-13}$ cm^2/s [24, 27], $K_g \approx 10^{-4}$ - 10^{-6} s^{-1} [28], and assuming $(P_s/c_s) \approx 1.5\times10^{12}$ Pa one can get for a bubble with the characteristic radius ~ 10 Å (i.e. $x_b \sim 10^3$) an estimation $q \geq 1$.

With further temperature increase q becomes >> 1 and the thermal resolution dominates over the radiation induced one. This corresponds to the linear dependence $N \propto x$ of the nodal line $dN/dt = 0$ at $x \leq x_b$ in the phase portrait of the system. In this case the critical nucleus size x_{cr} corresponding to the intersection of the nodal lines $dN/dt = 0$ and $dx/dt = 0$ (determined by the equation $N = 2\gamma(x\Omega)^{2/3}/kT \approx xP_e\Omega/kT$), can be evaluated as $x_{cr}^{1/3} \approx 2\gamma/[c_g(P_s/c_s)\Omega^{1/3}]$, thus, it increases with the decrease of c_g and exceeds the interatomic distance at relatively high values of $c_g \leq 10^{-2}$.

With further decrease of c_g the critical point approaches the other intersection point of the nodal lines (which determines the steady size of bubbles, see section II.3), Fig.5, and finally coincides with this point, Fig.6. This situation corresponds to the final state of the bubble system evolution, stabilised with respect to both the bubble size and density number under the steady irradiation conditions (see below). The condition of the two critical points coincidence can be evaluated from the relationship $q(x_{cr}) \sim 1$, that is $c_g^* \approx K_g\gamma^2\Omega/D_g kT(P_s/c_s)]^{1/2}$, therefore, at T ≈ 1500°C $c_g^* \approx 10^{-3}$ - 10^{-4}, and the corresponding critical bubble size $x^* \approx 10^2$ - 10^3.

With temperature increase in the range from 1500 to 1800°C the diffusion coefficient D_g increases approximately by one order of magnitude, leading to the critical bubble radius $r^* \propto x^{*1/3}$ increase by a factor of 3-5. In reality the observed increase of the bubble radius is smaller (≈ 1.5 times) [18], this apparently can be

explained by the unaccounted Arrhenius dependence of the factor (P_s/c_s) on temperature in Henry's law for the solid solute of the gas atoms.

It is easy to understand that the bubble system state characterised by the coinciding critical points in Fig.6 really corresponds to the final quasi-stationary state. Indeed, since the range of the bubble size growth (between points III and I in Fig.5) reduces to zero (Fig.6), the bubble radius is completely stabilised. On the other hand, since this radius simultaneously corresponds to the critical nucleus and significantly exceeds the interatomic distance, the probability of new bubbles generation at this stage is exponentially small. Moreover, if one assumes that after some long period of time new bubbles nevertheless appear, the subsequent reduction of the gas atom concentration c_g leads to the separation of the nodal lines (dashed line in Fig.6) and disappearance of the critical point (i.e. the critical nucleus size). In its turn, this immediately leads to the initiation of the bubbles resolution, c_g increase, and the recreation of the initial state of the system. [It is worthwhile to note that such a state is rather similar to the state described by the Lifshitz - Slyozov point in the theory of the late stage precipitation and coagulation in solid solutes [29]]. Therefore, the given quasi-stationary state is stable and corresponds to a late stage of the steady irradiation when all the generated fission gas atoms diffuse to the grain boundaries without trapping by the stabilised (with respect to the bubble size and number) system of the intergranular bubbles.

IV.2. Nucleation mechanism at high temperatures

In the preceding stage of the irradiation the mechanism of the bubble formation also differs from that at lower temperatures (T ≤ 1500°C). Indeed, since at high temperatures the critical nucleus size exceeds the interatomic distance in a rather wide range of values $c_g \le 10^{-2}$, small bubbles ($N = 2$) are «subcritical» (i.e. unstable) and disintegrate, practically during all the period of irradiation. The formation of larger (critical and «supercritical») bubbles occurs with some activation energy according to Volmer - Zeldovich mechanism [29]. Correspondingly, the bubble nucleation process at T ≥ 1500°C becomes heterogeneous and, thus, can be associated with the increased efficiency of fission particle tracks as probable nucleation sites (this is in accordance with electron microscope observations of the increasing amount of bubbles on the tracks at temperatures above 1500°C [18]). Naturally, under such conditions the description of the bubble formation by the constant nucleation factor F_N becomes invalid, since the correct description has to be based on the calculation of the activation barrier E_a for the fluctuation formation of the critical nucleus, $F_N \propto \exp(-E_a/kT)$.

V. Intergranular porosity

As in the case of the intragranular porosity (see section II.1), the evolution of the intergranular porosity is usually considered in the quasi-stationary approximation of mechanically equilibrium bubbles (e.g. [1-3, 9, 30, 31] . Such an approximation is based on the theoretical work [32], in which kinetics of the intergranular bubble growth determined by the diffusional flux of the grain boundary vacancies, was considered. According to [32], the grain boundary vacancy flux is evaluated as:

$$J_{g.b.} \approx (2\pi w/L) D_v^{g.b.} (c_v^{eq} - c_v(\rho)) = (2\pi w/L) D_v^{g.b.} c_v^{eq} \{1 - \exp[(P - P_h - 2\gamma/\rho)\Omega/kT]\} \approx$$

$$\approx - (2\pi w/L) D_u^{g.b.} (P - P_h - 2\gamma/\rho)\Omega/kT, \qquad (19)$$

where $D_v^{g.b.}$ is the grain boundary vacancy diffusion coefficient, $D_u^{g.b.} = D_v^{g.b.} c_v^{eq}$ is the grain boundary self-diffusion coefficient, w is the boundary thickness, ρ is the radius of curvature of the pore, $L \sim 1$ is a function of the fraction of the grain boundary area occupied by pores; thus, the quasi-stationary state ($J_{g.b.} = 0$) corresponds to the mechanically stable bubble:

$$P - P_h - 2\gamma/\rho = 0. \qquad (20)$$

However, applying these results to the UO_2 fuel it was generally ignored that the original model [32] did not consider an irradiated crystal. Under non-equilibrium conditions of the irradiated crystal the vacancy concentration in the bulk of the grain may be so high that the vacancy flux J_g from the interior of the grain to the boundary exceeds the grain boundary vacancy flux $J_{g.b.}$.

In order to determine the applicability range of the standard approach, one should compare the two fluxes. In accordance with Eq. (4):

$$J_g = 4\pi\rho D_v c_v\{1-(\beta_i/\beta_v)-(c_v^{eq}/c_v)\exp[(P-P_h-2\gamma/\rho)\Omega/kT]\}$$

$$\approx 4\pi\rho D_v c_v^{eq}[(1-\beta_i/\beta_v)(c_v/c_v^{eq})-1-(P-P_h-2\gamma/\rho)\Omega/kT], \qquad (21)$$

thus, the ratio of the two fluxes is:

$$J_{g.b.}/J_g \approx (D_u^{g.b.}/D_u)(w/\rho)[(P-P_h-2\gamma/\rho)\Omega/kT\,]/[1-(1-\beta_i/\beta_v)(c_v/c_v^{eq})+(P-P_h-2\gamma/\rho)\Omega/kT]. \qquad (22)$$

As demonstrated above, at T ≥ 1500°C the radiation effects become negligible (in comparison with the thermal ones), and $(1-\beta_i/\beta_v)(c_v/c_v^{eq}) \approx 1$. Therefore, since the value $(D_u^{g.b.}/D_u) \approx 10^5$ is extremely large [33], $J_{g.b.}/J_g >> 1$ and the approach of [32] can be reliably extended also to the case of the irradiated fuel at T ≥ 1500°C.

However, at lower temperatures, T < 1500°C it becomes $(1-\beta_i/\beta_v)(c_v/c_v^{eq}) > 1$, thus, $J_g \neq 0$ when $P - P_h - 2\gamma/\rho = 0$, and the above mentioned quasi-stationary condition $J_{g.b.} = 0$ leads to $J_{g.b.}/J_g \to 0$. This means that in reality the bubble state determined by the capillarity relation Eq. (20) is not stationary but corresponds to the bubble growing due to the diffusional flux of the point defects from the bulk of the grain. Therefore, for instance, at 1200°C when $(1-\beta_i/\beta_v)(c_v/c_v^{eq}) \geq 10$, for large bubbles with $\rho \geq 10^3$ Å the condition $J_{g.b.}/J_g > 1$ is valid only at $P - P_h \geq 10\times(2\gamma/\rho)$, whereas for $\rho \geq 1$ μm — only at $P - P_h \geq 10^2\times(2\gamma/\rho)$.

It is quite clear that in such a situation both processes of the bulk and grain boundary point defect diffusion should be considered self-consistently in order to describe the evolution of large intergranular bubbles (with $\rho >>$ 100 Å). Such a consideration shows that already at 1300-1400°C the bulk diffusion starts to dominate, this allows the description of the large intergranular bubble evolution by a line of the type represented by the dashed line in Fig.3. Indeed, since the internal pressure in such bubbles is rather small (in comparison with the capillary one, see section II.3.b), then, as seen from Eq. (22), the grain boundary vacancy flux turns to be really negligible in comparison with the bulk one. Hence, for instance, at 1300°C, $[(2\gamma/\rho) - P]\Omega/kT \approx (2\gamma/\rho)\Omega/kT \approx 10^{-2}$ for $\rho \approx$ 1 μm, therefore, $J_{g.b.}/J_g \approx 10^{-1}$. With temperature decrease the maximum size of the bubbles growing by the grain boundary diffusional mechanism also quickly decreases. Thus, at temperature below 1100°C the growth of all the intergranular bubbles with $\rho >$ 100 Å can be described neglecting the grain boundary vacancy diffusion flux, i.e. the standard approach based on the equilibrium crystal model [32] is not valid in this temperature range.

Since in this case (corresponding to the dashed line in Fig.3) the kinetics of the bubble size growth are determined by the point defect flux rather than the gas atom flux (as it was in the standard approach, see section II.3.b), the bubble growth rate becomes significantly higher. For the same reason, the internal pressure in such bubbles is rather low (in comparison with the capillary one). Both these factors can lead to the significant underestimation of the value and rate of the fuel swelling by the standard models, and can radically change the behaviour of the system even qualitatively. For instance, during formation of the open porosity on the grain faces, the channels formed by the bubble chains will practically conserve their form after the gas release from these bubbles (see dashed-dotted line in Fig.3) and will not shrink (as in the models for the "capillary" bubbles, e.g. [9]). This in its turn will additionally increase the gas release rate from the fuel.

VI. Conclusions

In the present paper the standard approaches for modelling of the inter- and intragranular bubbles evolution in the UO_2 fuel are critically analysed on the basis of the available experimental data. It is demonstrated that the main source of errors in the simplified treatment of the problem by the standard models can be associated with the underestimation of:

- the radiation effects at temperatures below ≈ 1500°C (where these effects dominate over the thermal ones);
- the thermal effects at temperatures above ≈ 1500°C (where these effects dominate over the radiation ones).

At low temperatures (≤ 1500°C) the generally accepted quasi-stationary approximation based on the capillarity relation for growing bubbles fails, since at these temperatures point defects generated in the fuel under irradiation conditions significantly change the behaviour of growing bubbles, especially in the case of large

bubbles formed on the grain faces or during transients in the bulk of the grains. In particular, this may lead to a significant underestimation of the value and rate of the fuel swelling. On the other hand, the presented analysis of the defect structure evolution allows quantitative description of the bubble nucleation mechanism, as well as evaluation of the bubble number density and stable size attained under steady irradiation conditions.

At high temperatures (≥ 1500°C) the thermal resolution of gas atoms from bubbles generally unaccounted in the standard models, becomes the dominant process leading to the significant increase of the critical nucleus of the bubbles and, as a result, change of the mechanism and kinetics of the bubble generation. On the other hand, self-consistent consideration of the thermal and radiation induced resolution processes allows natural explanation and quantitative description of the bubble size and number stabilisation observed also at high temperatures under steady irradiation conditions.

References:

1. J. Rest, GRASS-SST: A Comprehensive, Mechanistic Model for the Prediction of Fission-Gas Behavior in UO_2 - base Fuels during Steady-state and Transient Conditions, - NUREG/CR-0202, ANL-78-53, 1978.
2. J. Rest, S.A. Zawadzki. FASTGRASS: A Mechanistic Model for the Prediction of Xe, I, Cs, Te, Ba, and Sr Release from Nuclear Fuel under Normal and Severe-Accident Conditions, - NUREG/CR-5840, ANL-92/3, 1992.
3. VICTORIA: A Mechanistic Model of Radionuclide Behaviour in the Reactor Coolant System under Severe Accident Conditions,- NUREG/CR-5545, 1992.
4. J.L Katz, H. Wiedersich, Nucleation of Voids in Materials, Supersaturated with Vacancies and Interstitials, - J.Chem.Phys., 1971, v.55, p.1414.
5. K.C. Russel, Nucleation of Voids in Irradiated Materials, - Acta Metall., 1971, v.19, p.753.
6. L.K. Mansur, M.H. Yoo, The Effect of Impurity Trapping on Irradiation Induced Swelling and Creep, - Journal of Nuclear Materials, 1978, v.74, p.228.
7. C.C. Dollins, F.A. Nichols, Swelling and Gas Release in UO_2 at Low and Intermediate Temperatures, - Journal of Nuclear Materials, 1976, v.91, p.143.
8. M.H. Wood, J.R. Matthews. A Simple Operational Gas Release and Swelling Model. - Journal of Nuclear Materials, 1980, v.91, p.35.
9. R.J. White, M.O. Tucker, A New Fission-Gas Release Model, - Journal of Nuclear Materials, 1983, v.118, p.1.
10. E.E. Gruber, The Role of Bubble-Size Equilibration in the Transient Behavior of Fission Gas, - ANL-78-36, 1978.
11. M.W. Finnis, M.R. Hayns, R. Bullough, The Response of Fission Gas Bubbles to Rapid Heating, - AERE-R-7970, 1975.
12. M.E. Gulden, Migration of Gas Bubbles in Irradiated Uranium Dioxide, - Journal of Nuclear Materials, 1967, v.23, p.30.
13. C. Baker, The Migration of Intragranular Fission Gas Bubbles in Irradiated Uranium Dioxide, - Journal of Nuclear Materials, 1977, v.71, p.117.
14. K.C. Russel, The Theory of Void Nucleation in Metals, - Acta Metall., 1978, v.26, p.1615.
15. A.D. Whapham, B.E. Sheldon, Electron Microscope Observation of the Fission-Gas Bubble Distribution in UO2, - Report AERE-R-4970, 1965.
16. R.M. Cornell, An Electron Microscope Examination of Matrix Fission Gas Bubbles in Irradiated UO_2, - Journal of Nuclear Materials, 1971, v.38, p.319.
17. A.J. Manley, Gas Bubbles and Porosity in Irradiated UO_2, - TRG Report 2539 (S), 1974.

18. C. Baker, The Fission Gas Bubble Distribution in Uranium Dioxide from High Temperature Irradiated SGHWR Fuel Pins, - Journal of Nuclear Materials, 1977, v. 66, p.283.

19. Yu.G. Degaltsev, N.N. Ponomaryov-Stepnoy, V.F. Kusnetsov, Behaviour of High Temperature Nuclear Fuel under Irradiation, -Moscow, 1987 (*in Russian*).

20. L.D. Landau, E.M. Lifshitz, Hydrodynamics, Moscow, 1986 (*in Russian*).

21. I.L.F. Ray, H. Thiele, Hj. Matzke, Transmission Electron Microscopy Study of Fission Product Behaviour in High Burnup UO2, - Journal of Nuclear Materials, 1992, v.188, p.90.

22. A.D. Brailsford, R. Bullough. The Theory of Sink Strengths, - Philosophical Transactions of the Royal Society, 1981, v. A302, p.87.

23. Hj. Matzke, Diffusion in Ceramic Oxide Systems, - Advances in Ceramics, 1986, v.17, p.1.

24. Hj. Matzke, Gas Release Mechanisms in UO_2 - A Critical Review, - Radiation Effects, 1980, v. 53, p.219.

25. R. Bullough, M.R. Hayns, The Effects of Temperature Changes on Void Swelling, - Journal of Nuclear Materials, 1975, v. 55, p. 237.

26. V.V. Surenyanz, Solutes of Inert Gases in Solids, - Zh. Fiz. Khimii, 1971, v. XLV, No.2, p.2985 (*in Russian*).

27. Hj. Matzke, Fundamental Aspects of Inert Gas Behaviour in Nuclear Fuels: Oxides, Carbides and Nitrides, - in Fundamental aspects of Inert Gases in Solids, Ed. By S.E. Donnelly and J.H. Evans, Plenum Press, New York, 1991, p. 401.

28. J.A. Turnbull, R.M. Cornell, The Re-Solution of Fission-Gas Atoms from Bubbles during Irradiation of UO_2 at an Elevated Temperature, - Journal of Nuclear Materials, 1971, v. 41, p.156.

29. E.M. Lifshitz, L.P.Pitaevsky, Physical Kinetics, Moscow, 1979 (*in Russian*).

30. M.O. Tucker, Relative Growth Rates of Fission-Gas Bubbles on Grain Faces, - Journal of Nuclear Materials, 1978, v. 78, p.17.

31. J.R. Matthews, M.H. Wood, A simple operational gas release and swelling model. - Journal of Nuclear Materials, 1980, v. 91, p. 241.

32. M.V. Speight, W. Beere, Vacancy Potential and Void Growth on Grain Boundaries, Metal Science, 1975, v. 9, p.190.

33. Alcock et al., Thermodynamics, IAEA Symposium Proceedings, Vienna, 1965, p. 57.

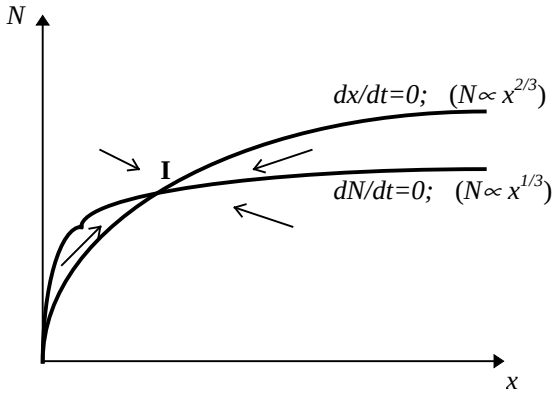

Fig.1: Schematic diagram of nodal lines in the simplest case of «capillary» bubble evolution. Velocity vectors and the critical point I (stable node) are indicated .

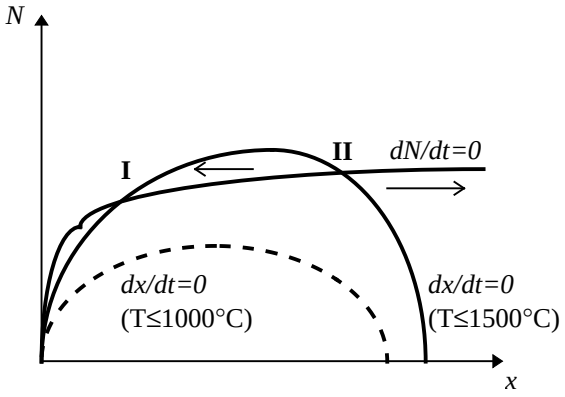

Fig.2: Nodal lines in the case of non-equilibrium crystal oversaturated with point defects. Two critical points I (stable node) and II (saddle point) are indicated.

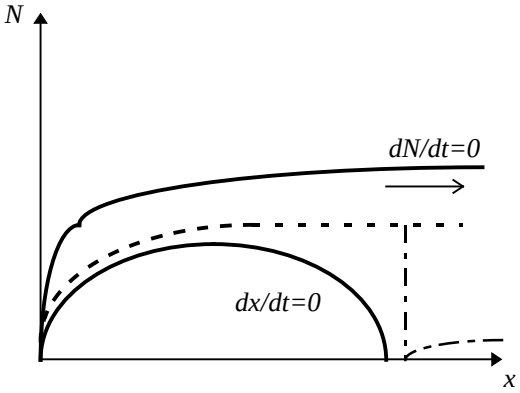

Fig.3: Nodal lines and trajectory of growing bubbles (dashed line) in the absence of critical points (corresponding to the low temperature case in Fig.2).

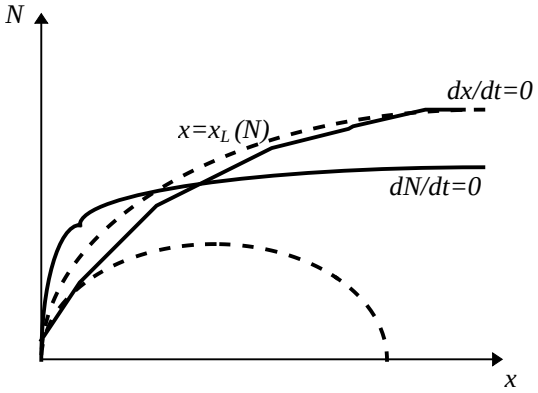

Fig.4: Nodal lines with account of the small bubble relaxation mechanism (leading to the transformation of Fig.3).

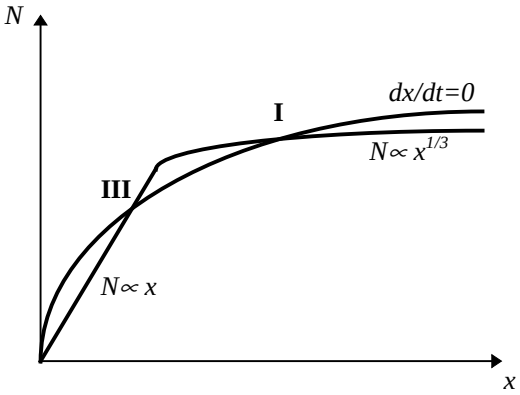

Fig.5: Nodal lines in the high temperature case (T≥1500°C) with account of the thermal resolution of gas atoms from bubbles. Saddle point III corresponds to the critical nucleus.

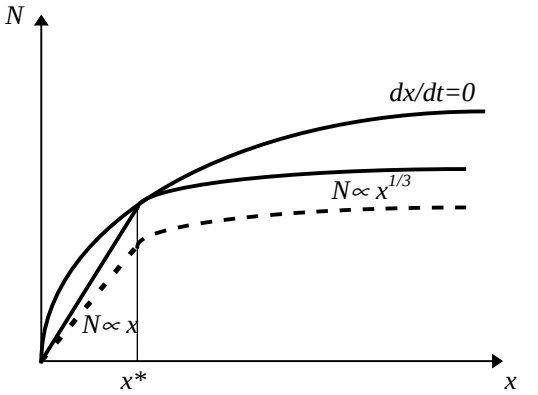

Fig.6: Nodal lines in the case of the two critical points I and III coincidence, corresponding to stabilisation of bubble size and number under steady state irradiation conditions at T≥1500°C.